Autonomous Guidance Algorithms for NASA Learn-to-Fly Technology Development

John V. Foster[1]
NASA Langley Research Center, Hampton, VA 23681-2199

Learn-to-Fly (L2F) is an advanced technology development effort under the NASA Transformative Aeronautics Concepts Program (TACP) that is aimed at assessing the feasibility of self-learning flight vehicles. Specifically, research has been conducted to demonstrate the potential to merge two enabling technologies; real-time aerodynamic modeling and adaptive controls, to substantially reduce the typical ground and flight testing requirements for air vehicle design. The approach to this effort involved development of unique airframes and on-board algorithms to demonstrate key L2F technologies on a fully autonomous flight test vehicle. This research, that included an aggressive flight test program, was intended to rapidly advance these technologies and demonstrate capabilities of the L2F approach. Key components of the L2F architecture include real-time aerodynamic modeling, adaptive controls and control allocation, and guidance. This paper provides an overview of the guidance algorithm which primarily served as an executive function to coordinate control commands for range navigation and the desired test conditions, provide autonomous envelope limiting/expansion and enable automatic landing to touchdown with no intervention from a human operator. A discussion of the L2F concept-of-operations and unique flight testing considerations, which influenced the guidance functional requirements, is included and results of recent flight testing are presented.

Nomenclature

AGL = above ground level
AOA = angle of attack
C_{lp} = non-dimensional aerodynamic roll damping parameter
C_{nr} = non-dimensional aerodynamic yaw damping parameter
$C_{n\beta,dyn}$ = non-dimensional static lateral-directional stability parameter
GPS = Global Positioning System
L2F = Learn-to-Fly
L/D = aerodynamic lift to drag ratio
LDG = landing
NASA = National Aeronautics and Space Administration
PTI = programmed test inputs
RA = radius of acceptance
R/C = radio control
RSO = Range Safety Officer
V_t = true airspeed
VCAS = calibrated airspeed
α = angle of attack
γ = airmass relative glide path angle

[1] Senior Research Engineer, Bldg 1232/Mail Stop 308, john.v.foster@nasa.gov, AIAA Associate Fellow

I. Introduction

Learn-to-Fly (L2F) is an advanced technology development effort under the NASA Transformative Aeronautics Concepts Program (TACP) as an element within the Convergent Aeronautics Solutions (CAS) project that is aimed at assessing the feasibility of self-learning flight vehicles. Specifically, research has been conducted to demonstrate the potential to merge two enabling technologies; real-time aerodynamic modeling and adaptive controls, to substantially reduce the typical ground and flight testing requirements for air vehicle design. The approach to this effort involved development of on-board algorithms and unique airframes to demonstrate key L2F technologies on a fully autonomous flight test vehicle. This research, that included an aggressive flight test program, was intended to rapidly advance these technologies and demonstrate key capabilities of the L2F approach. An overview of the L2F project is provided in Ref. [1].

An illustration of the L2F system architecture is shown in Fig. 1. Key components include real-time aerodynamic modeling, adaptive controls and control allocation, and guidance. A description of the hardware and concept of operations is presented in Ref. [2]. The real-time aerodynamic modeling function is described in Ref. [3] and the control law is discussed in Ref. [4]. This paper provides an overview of the guidance algorithm which primarily served as an executive function to coordinate control commands for navigation and the desired test conditions, provide autonomous envelope limiting/expansion and enable automatic landing to touchdown with no human operator intervention. Section II will present the concept-of-operations relative to the guidance algorithm and discuss the issues associated with range safety for an autonomous/self-learning vehicle. Section III will provide a functional description of the guidance algorithm components including navigation within the test range, autonomous envelope monitoring concepts, and the autonomous landing approach used for the test vehicles. Section IV will present results from recent flight tests of the primary unpowered testbed (Woodstock) and a conventional powered airframe (E1) that are described in Ref. [2].

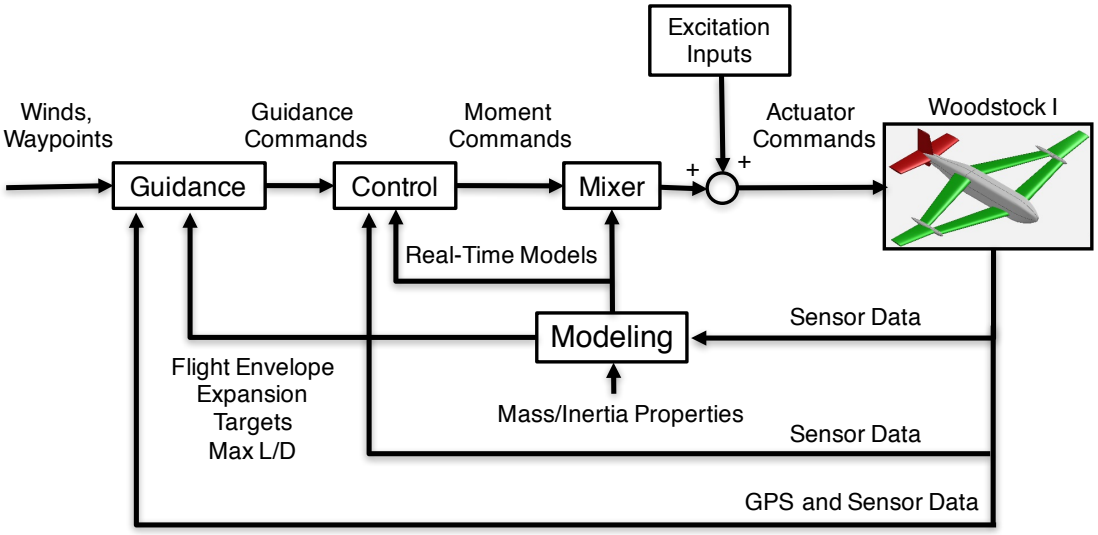

Fig. 1. L2F system architecture.

II. Concept of Operations

The L2F concept-of-operations introduced several flight testing considerations unique to self-learning flight test vehicles which influenced many of the requirements for the guidance algorithms. The baseline flight profile, illustrated in Fig. 2, was designed to allow full autonomous flight from launch to landing with no external control. The L2F vehicle was dropped from a tethered balloon by a radio-controlled manual release mechanism[2]. Following release from the balloon, the maneuvering sequence was designed to establish stabilized flight path control as quickly as possible. A pull-up maneuver was initiated to acquire near 1g stabilized flight while simultaneously starting self-learning (via real-time aerodynamic modeling) and navigation within the test range. At this point the

guidance algorithm began to provide the target values of angle of attack and sideslip angle to the control system to expand the flight envelope for real-time modeling. During this phase of the flight profile, multi-frequency control surface commands, known as programmed test inputs (PTI) were used to excite the vehicle to generate informative data that would allow estimation of the aerodynamic model. This model was in turn used by the closed loop controller to maintain desired flight conditions. Based on the available altitude, the sequence of aerodynamic model identification and closed-loop control continued as the vehicle navigated within the test range. Various envelope protection features, such as angle of attack (AOA) limiting and airspeed limiting were triggered as needed. At a pre-defined altitude, the control algorithm switched to an autoland system that provided maneuvering commands to landing based on an energy management approach.

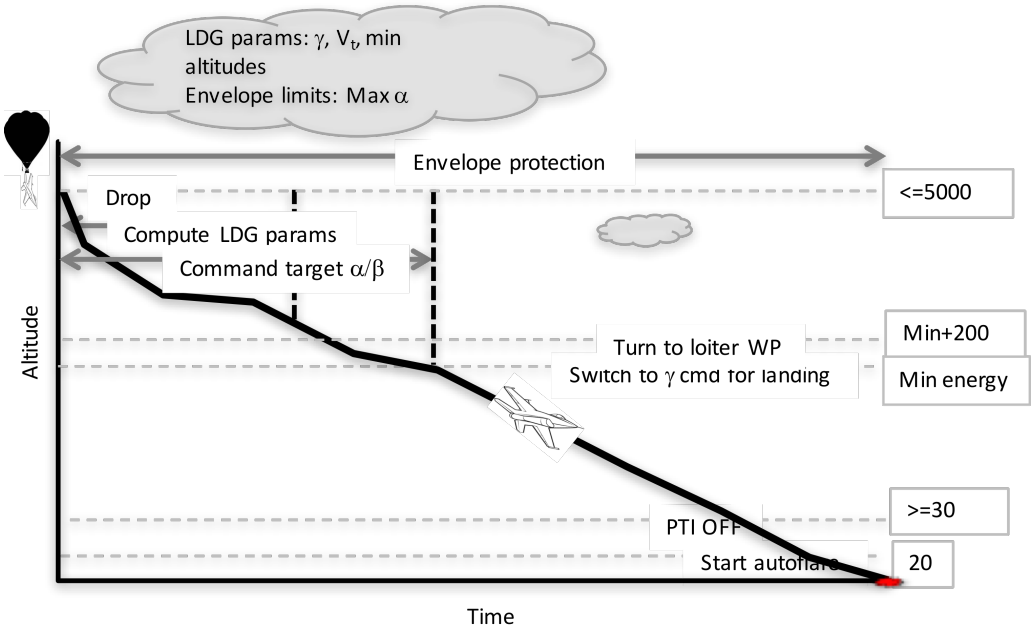

Fig. 2. Baseline L2F flight profile.

III. Guidance Algorithm Functional Descriptions

The purpose of the guidance algorithm was to serve as an executive function to coordinate control commands for executing the flight profile described above. The primary functional requirements for the guidance algorithm were as follows:

- Maintain flight path within a defined test area (ground track command)
- Provide guidance commands for the desired test conditions (angle of attack, sideslip angle)
- Provide limited envelope protection (maximum angle of attack and minimum airspeed)
- Provide flight path control commands for autonomous landing to a target area with minimal vehicle damage (ground track, glidepath commands)

The approach to designing the guidance algorithm was through the use of simulation tools as described in Ref. [1]. Low fidelity vehicle simulations were used as surrogates to allow development of the L2F onboard control software and develop the flight test procedures. A functional diagram of the guidance algorithm is shown in Fig. 3. The following sections provide detailed discussions of the requirements for test range navigation, autonomous envelope limiting/expansion, and autonomous landing.

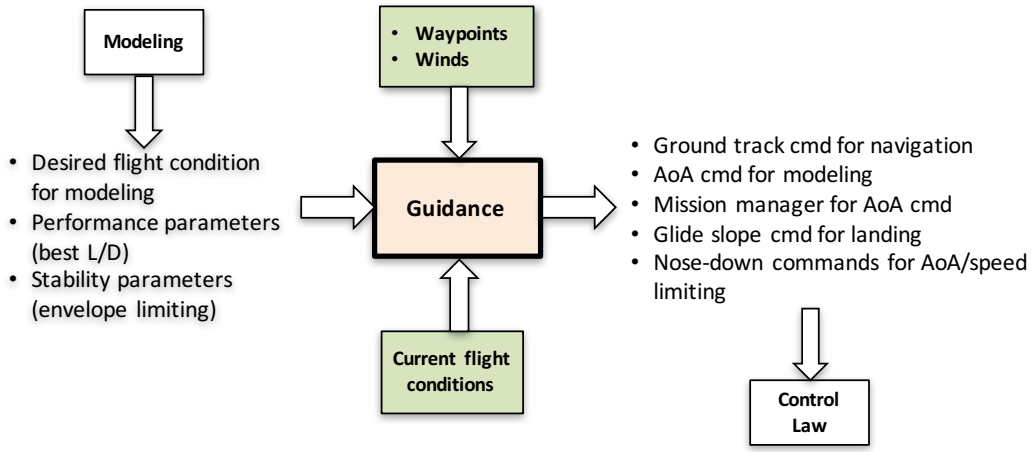

Fig. 3. Guidance algorithm functional description.

Test Range Navigation

The L2F flight test vehicles were operated in controlled test ranges, including Restricted airspace. The Woodstock (unpowered) vehicles were launched from a tethered balloon using a radio control (R/C) release mechanism. The concept of operations was designed to allow launch from altitudes up to 5000 ft above ground level (AGL). However, the permissible launch altitude could be limited by other considerations such as balloon ground equipment positioning, the safety pilot's line of sight, or wind limits. The advantage of launching at higher altitudes was to allow maximum time for data acquisition and control learning during the flight. The E1 (powered) aircraft was operated from a hard surface runway and manually flown by the safety pilot for the takeoff, climb to test altitude and landing. The flight/ground hardware and the method of test operation for the test vehicles is discussed in detail in Ref. [2].

For range navigation, Global Positioning System (GPS) waypoint tracking was chosen due to the availability of onboard avionics and ease of implementation at any test location. The outer loop control algorithm, part of the Control block shown in Fig. 2, was designed with ground track command, and the desired ground track was computed simply as the vector from the current vehicle position to the desired GPS waypoint. The test pattern was typically designed as a rectangular box, and the latitude/longitude for each waypoint was pre-loaded in the flight software before each flight. The guidance function included logic to sequence through the waypoints in a pre-defined order and repeat the waypoint sequence as altitude allowed. The logic for waypoint passage used the radius of acceptance (RA) to trigger sequencing to the following waypoint. The RA was a pre-defined value, which was the minimum radial distance to the waypoint that defined waypoint crossing while allowing some error in tracking accuracy. One of the risks to this approach was the possibility of the vehicle overshooting a waypoint due to winds or degraded tracking performance caused by control limitations. For the flight tests described in this paper, 200 ft was used as the RA to allow an adequate margin for tracking error. Other waypoint crossing criteria are discussed in the literature but were not considered for this research.

The safety pilot was provided direct control to the vehicle via an independent R/C link and hand-held transmitter. However, due to the unknown flying qualities of the L2F vehicles, there were no assurances that the safety pilot could adequately control the vehicle during any phase of flight, including landing. Therefore, the safety pilot's primary role was for range containment in the event the vehicle lost navigation capability and could potentially exit the test range. The safety pilot was required to maintain positive awareness of range positioning, either by visual line-of-sight or via an independent range display (Woodstock vehicles only). The safety pilot, or Range Safety Officer (RSO), could call for flight termination which could be accomplished by application of pro-spin control inputs either by manual inputs from the safety pilot or from the pre-programmed onboard receiver that would be activated in the event of lost R/C link.

The flight test area was designed to allow a safety pilot to maintain visual line-of-sight or positive positioning, while the vehicle navigated between fixed waypoints prior to landing at a target touchdown area. An important consideration for test range layout was contingency management in the event of a failure that could lead to the vehicle exiting the test range. A common contingency management approach is to provide adequate lateral area for the vehicle to remain within the test range for a maximum glide condition to ground impact. Since the

maximum glide performance, as defined by lift-to-drag ratio (L/D) was not known prior to flight, estimates were used with a margin of safety applied.

The test envelope limits of concern for the flight test were winds aloft, visibility and cloud clearance, and maximum crosswind for landing. The winds aloft were considered a primary limit for waypoint navigation accuracy due to the potential excessive deviations while tracking to a waypoint. In addition, significant variations in airspeeds were expected. Due to the anticipated low airspeeds of the test vehicles, and analysis of simulation-based flight profiles, a maximum wind velocity of 20 kts was considered a suitable limit for all test vehicles. The inflight visibility requirement was due to the need for the safety pilot to maintain visual line of sight at all times. Typical visibility limits were no less than one mile and remaining clear of clouds. Lastly, crosswind landing limits were considered to prevent controllability problems and possible model damage for landing. Based on simulation analysis, 10 kts was used as the maximum crosswind landing limit.

Another important consideration for designing range operational limits was the maximum lateral drift during a flight termination event. Due to the potential for the vehicle to exit the test range due to flight termination, impact point prediction software[6] was used to estimate the lateral drift in the presence of winds in a fully-developed spin. Based on the estimated drag coefficient at an angle of attack typical of a spin, this algorithm was used to define the lateral range boundaries for worst-case wind conditions. In addition, the range boundary design also took into account the heading and forward speed at the point of termination.

Autonomous Envelope Expansion

An important consideration for flight testing of the L2F concept is that the normal flight envelope is unknown prior to flight. For the purposes of this discussion, the normal flight envelope is defined as the set of flight conditions where stable, controlled flight can be maintained at the desired test conditions. Therefore, a unique challenge of the L2F concept is that the normal envelope must be identified concurrently as the aerodynamic model is identified in flight, based on flight data. For example, normal flight conditions, such as the angle of attack for 1g steady flight, or maneuvering boundaries, such as aerodynamic stall, are unknown. The concept of autonomous envelope expansion was addressed in this project and some of the requirements and concepts were evaluated as part of this research. However, a comprehensive demonstration of this concept was not completed and remains an area for further research.

One of the biggest risks in flight testing of L2F vehicles was inadvertent loss of control. Unlike more typical flight testing, where estimates of vehicle stability boundaries are often available, no estimates of loss of control susceptibility were available for the L2F vehicles. In the event of loss of control, the ability to navigate within the test range may be compromised, leading to range boundary violations or flight termination. Furthermore, recovering from a loss of control event and returning to the normal flight envelope posed a critical challenge from a modeling and controls standpoint. This risk led to a research objective to predict/anticipate stability boundaries and identify control strategies to prevent or recover from a loss of control event. However, reliable aerodynamic modeling can only be achieved if the vehicle operates at the flight condition of interest for a sufficient amount of time (Ref. [3]). Therefore anticipation of loss of control is really an extrapolation of the modeling results and can be difficult to do accurately. In addition, in the event of loss of control, identification of the aerodynamic model and providing the correct control response, especially during highly-dynamic motions, is a significant challenge.

For the first phase of flight testing, a simplified approach to envelope expansion was chosen. The guidance algorithm computed the desired angle of attack via an open-loop saw-tooth function such that the commanded angle of attack varied slowly to allow adequate time for model identification. The peak angle of attack, along with the rate of change, was predefined for each flight, and was intended to be changed using a build-up approach. The maximum angle of attack ranged from 5-10° and the time rate of change of the angle of attack ranged from 0.2 to 0.5°/sec. By controlling and monitoring angle of attack, stall prevention could be achieved by limiting AOA to preset values or by predicting and avoiding the potential stall condition. For example, due to the increased potential for stall/departure during turning flight, the commanded angle of attack was reduced while turning near waypoints.

The approach of stall avoidance does not guarantee that a loss-of-control event will not occur but likely lowers the risk. The concept of anticipating loss of control boundaries by using pre-defined metrics was considered. Candidate metrics included damping derivatives (e.g. C_{lp} C_{nr}), static stability derivatives such as $C_{n\beta,dyn}$, and control surface saturation that were investigated as part of the envelope limiting logic. Of concern with this approach is the reliability of computed metrics causing a false-positive envelope limitation or not detecting a potential loss of control. For the purposes of this flight test, the feasibility of using modeling-based metrics was investigated but the development of robust criteria remains a topic for future research.

For the current L2F flight testing, a simple AOA and airspeed envelope limiting algorithm was evaluated. An illustration of the control logic is shown in Fig. 4. The minimum threshold airspeed was selected prior to the flight based on known stall speeds of similar sized vehicles. During flight, the airspeed was continuously monitored and if it was lower than the minimum threshold, a low AOA was commanded resulting in an increase in airspeed. A deadband function was included so that the nose-down command remained until the airspeed increased by a pre-defined value, thus allowing for a complete recovery back into the desired airspeed envelope.

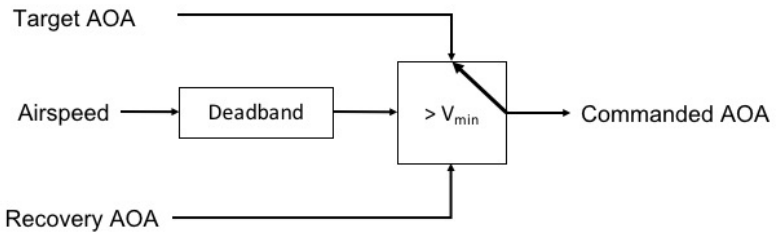

Fig. 4. Logic for AOA and airspeed envelope limiting.

Autonomous Landing

As previously stated, it was assumed unknown if the vehicle's piloted flying qualities were adequate for a safety pilot to precisely maneuver or land the vehicle without damage. Therefore, an autonomous landing algorithm (autoland) was integrated within the guidance function. The landing pattern was defined by seven waypoints which are illustrated in Fig. 5. The latitude and longitude of each waypoint was computed in flight to allow the algorithm to be rapidly adapted for any runway location or orientation. The landing was initiated by proceeding to a loiter point from the rectangular pattern at a predefined altitude. The purpose of this maneuver was to ensure the vehicle was in the safety pilot's line of sight and in an energy state sufficient for landing. The loiter point was typically directly overhead the designated landing point. From the loiter point, the landing pattern comprised a downwind leg, base leg, and final approach to the target landing area. An intermediate waypoint on the final approach was included to improve runway lineup and an overshoot waypoint was included to ensure continued guidance in the event the vehicle overshot the landing area.

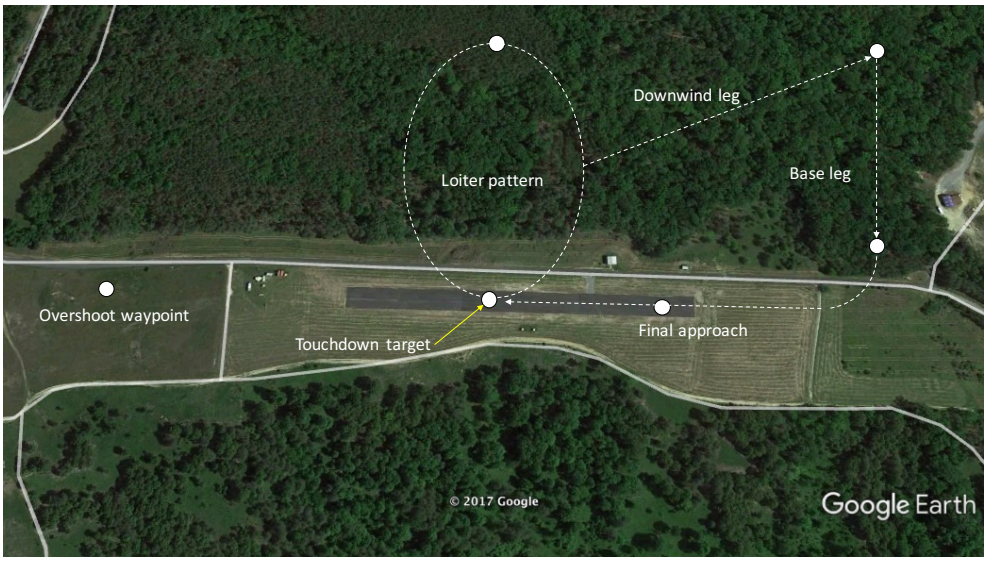

Fig. 5. Waypoint pattern for autonomous landing.

Since the Woodstock L2F vehicles were unpowered, an energy management approach was used to provide target altitudes for each waypoint in the landing pattern. The vehicle's pitch controller switched to a flight path

command system and landing approach was flown at a constant airmass flight path angle (γ). Using pre-loaded estimates for wind speed and direction, and onboard computed trim airspeed, target altitudes were computed real-time in flight for fixed waypoints which would allow the vehicle to glide to a target touchdown point. Due to the potential for inaccuracies in controlling flight path, waypoint skipping logic was used to manage energy by advancing the navigation fix to the following waypoint if the vehicle reached the minimum energy altitude prior to crossing the current waypoint in the landing pattern. As illustrated in Fig. 6, the commanded flight path angle was computed from estimates of best L/D and the corresponding true airspeed was computed from the estimated lift curve which were outputs from the real-time aerodynamic modeling function. This approach served to demonstrate self-learning of an optimal performance landing strategy.

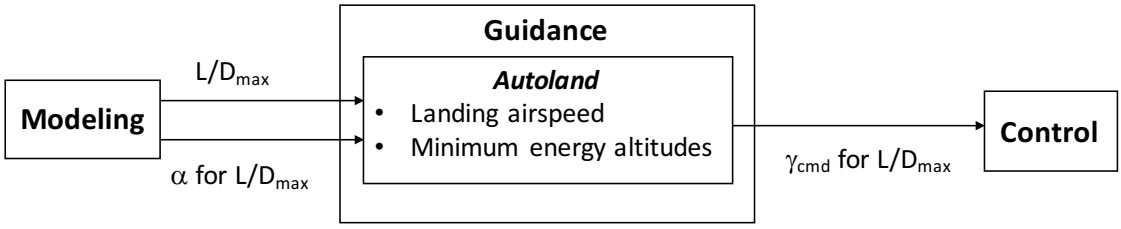

Fig. 6. Autoland inputs/outputs.

The Woodstock test vehicle was designed with rigid landing skids for the purpose of minimizing weight and complexity from landing gear. Therefore, airframe structural loads during landing were important design considerations for the autoland algorithm, so that the vehicle would sustain minimal damage at touchdown. Due to the position of the air data probe near the vehicle nose, pitch attitude at touchdown was also considered. Touchdown position accuracy and line of sight was important in the event the safety pilot was required to take control during the landing flare. While several test ranges were considered during the L2F test program, including runway lengths as short as 1200 ft, landing criteria were defined as follows;

- Desired/adequate touchdown location relative to fixed target: +/-200 / 500 ft
- Rate of descent at touchdown: < 5 ft/sec
- Bank angle: < +/- 15 deg
- Pitch attitude: >0 deg, <10 deg

The autoland algorithm used a laser altitude sensor for primary altitude feedback during autoflare. Due to the range limits of the laser sensor, barometric altitude was used as the primary altitude sensor until descending to an altitude of 30 ft AGL, at which point the autoland system switched to the laser-based altitude sensor. To prevent the potential for a wingtip strike, the commanded heading was held constant below 15 ft AGL so that the wings returned to a near level attitude. Finally, a nose-up command proportional to height AGL and rate of descent was used to increase pitch attitude for touchdown. During the L2F control system development, simulation was used in a Monte Carlo fashion to assess landing performance using the above criteria. An example of the ability of the autoflare algorithm to arrest the rate of descent and achieve the desired roll attitude at touchdown is illustrated in Fig. 7.

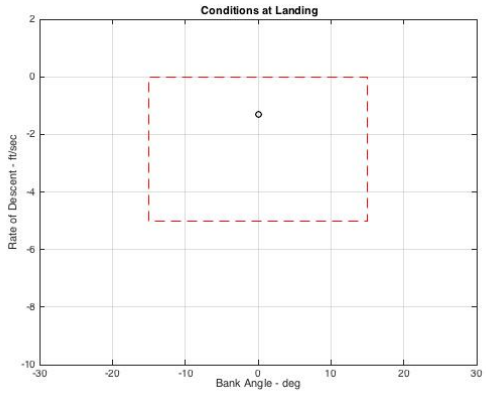

Fig. 7. Simulation criteria for autoflare performance. Red dashed boundary indicates desired conditions at touchdown.

A simulation time history illustrating the envelope protection and autoflare functions is shown in Fig. 8. In this figure, an example of the airspeed recovery logic is shown at t=25 sec. Upon decelerating to 25 kts, the recovery logic provides a nose-down control input and the airspeed is seen to increase by 10 kts. Secondly, the autoflare function is shown starting at t=45 sec. Starting from a stabilized descending flight path, an increased (nose up) pitch attitude is commanded to arrest the rate of descent and establish the desired attitude at touchdown.

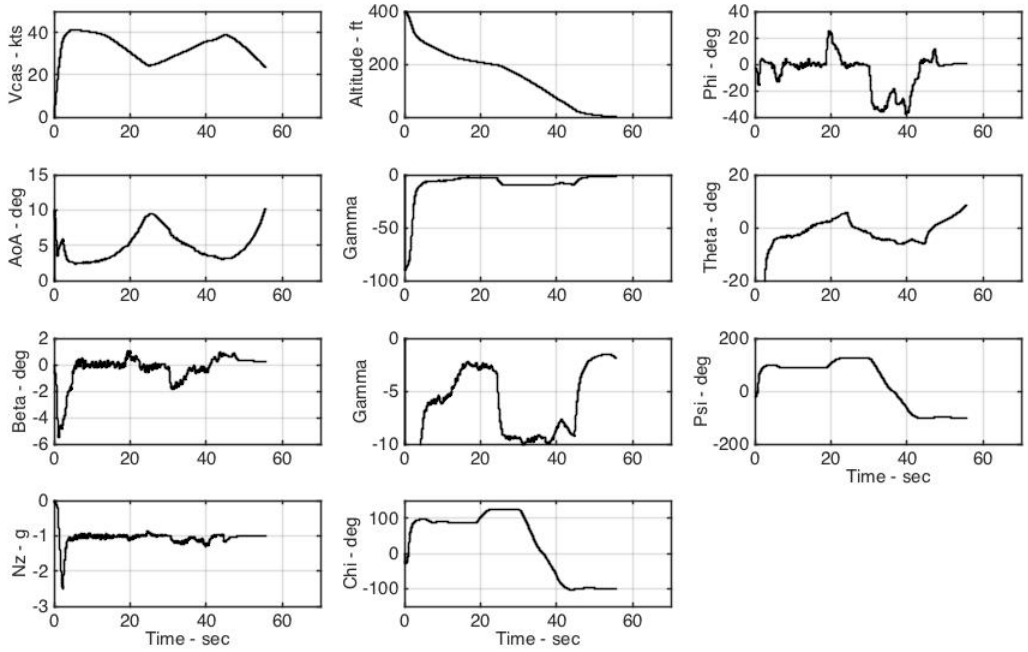

Fig. 8. Simulation time history illustrating envelope protection and autoland from low-altitude release. Airspeed recovery logic occurs at t=25 sec. Autoflare starts at t=45 sec.

IV. Flight Test Results and Discussion

Flight testing of the L2F concept was conducted during three deployments using various test vehicles (Ref. [1], [2]). This paper presents results from the latest deployment where a unique unpowered airframe (Woodstock)

was tested along with a surrogate conventional powered airframe (E1). As reported in Ref. [1], Woodstock flight tests resulted in the loss of both vehicles such that the feasibility of the L2F modeling and control algorithms could not be demonstrated. However, limited modeling data was acquired, albeit at out-of-envelope conditions that served to illustrate the need for and complexities of autonomous envelope limiting. Eleven successful flights were completed on the E1 aircraft which was used to develop and demonstrate various components of the onboard avionics and algorithms, including the guidance algorithms, and for risk reduction for the Woodstock flights. The following sections include discussions of waypoint navigation and autoland energy management for the E1 aircraft test flights. The challenges of autonomous envelope monitoring are discussed using test data from both the Woodstock and E1 aircraft.

Waypoint Navigation

Flight tests of the E1 test vehicle were conducted to demonstrate navigation performance concurrent with real-time aerodynamic modeling and control functions. The first flight profile involved navigation between two waypoints where ground track commands were started four seconds following the start of the real-time modeling and then allowing the vehicle to navigate to the first waypoint in the sequence. Figure 9 shows the ground track during powered autonomous navigation between two waypoints that illustrated the ability to rapidly achieve accurate ground tracking performance and where waypoint crossing accuracy within 20 ft was demonstrated.

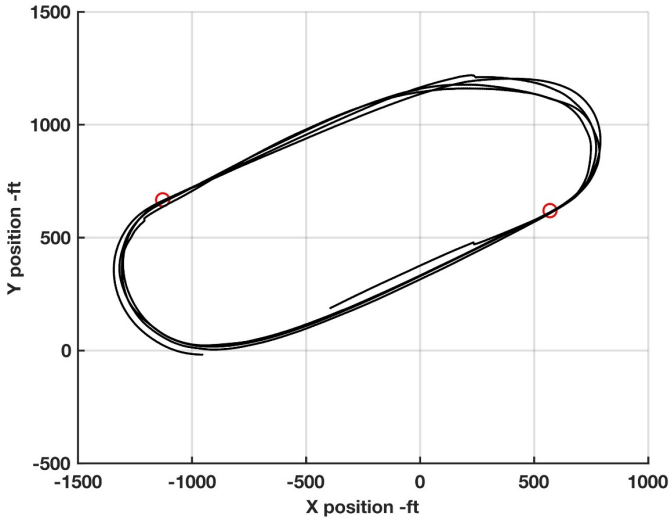

Fig. 9. Waypoint navigation performance. E1 aircraft, flight 5. Red symbols denote waypoint locations.

Autonomous Stability Monitoring

As previously discussed, the concept of stability monitoring and envelope limiting was considered primarily for the purpose of risk reduction. Currently there are no known validated metrics for this purpose therefore the identification of proposed metrics and logic was a research area for the L2F concept. One objective of these flight tests was to assess the feasibility of using real-time aerodynamic stability estimates for envelope limiting possibly leading to further research on envelope monitoring concepts. For these flight tests, envelope limiting logic using stability monitoring was not integrated in the guidance algorithm but various postulated metrics were analyzed post flight.

Figure 10 shows time histories of selected static and dynamic lateral-directional stability parameters from the E1 and Woodstock flight tests. The rate damping parameters, C_{lp} and C_{nr} , and the static stability criteria $C_{n\beta,dyn}$ are open-loop aerodynamic stability metrics that are often used to provide an indication of potential loss of control boundaries. These metrics only represent the bare airframe stability and therefore would not be directly applicable to closed-loop instabilities.

Figure 10(a) shows E1 test data from a flight profile designed to emulate the Woodstock flight profile. For the first two seconds, an instability is indicated likely due to the initial high AOA conditions, however no instabilities are indicated after 2 sec and the AOA remains near the commanded value. In contrast, Fig. 10(b) shows test results for Woodstock where stable conditions are indicated for the first two seconds but a rapid divergence in

the AOA is indicated at 2 seconds into the flight, concurrent with unstable values of yaw damping. The AOA is significantly higher than the commanded value indicating a loss of control event which in this case was likely a fully developed spin throughout the remainder of this time history. It is noteworthy that positive roll damping and weak yaw damping is indicated after 10 sec and the $C_{n\beta,dyn}$ parameter indicates positive static stability throughout the flight after 14 sec.

These examples illustrate the difficulty in applying real-time metrics in highly dynamic flight conditions, in time to anticipate the loss of control and provide corrective inputs. The accuracy of these data shown in the figures cannot be determined due to the lack of validated ground test data; however, the potential accuracy and limitations are discussed in Ref. [3]. For a practical implementation of this approach, it is recognized that a time delay in the real-time modeling results is inherent in the on-board algorithm, and therefore this approach may not provide suitable anticipation of approaching loss-of-control boundaries, especially for very abrupt loss of control events. This time delay arises from the simple fact that an accurate model can only be identified from the data after the behavior to be modeled has been exhibited in the data. Note that this only applies to the first time the modeling algorithm encounters a particular flight condition, and not subsequent encounters. The traces of AOA suggest that perhaps metrics that monitor the difference between commanded and actual flight conditions should be considered and may provide a more direct prediction of degraded control. Another possibility would be to monitor the rate of change of stability and control parameter estimates, and their proximity to loss-of-control boundaries.

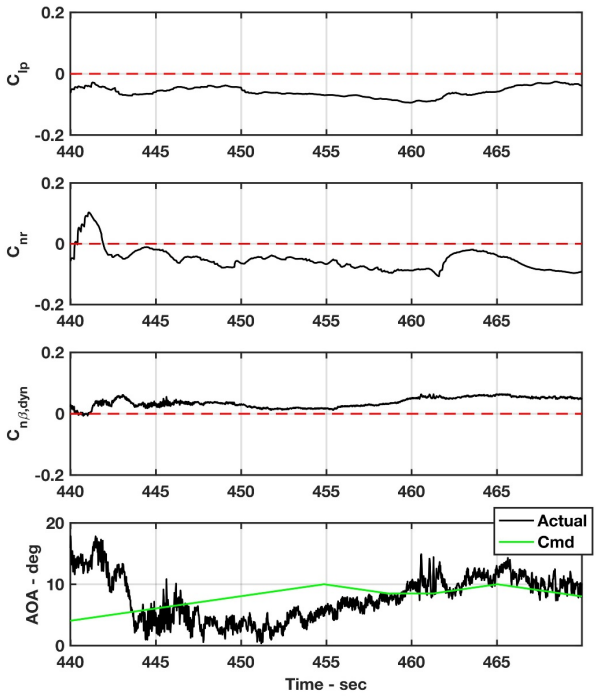

(a) E1 aircraft, flight 8.

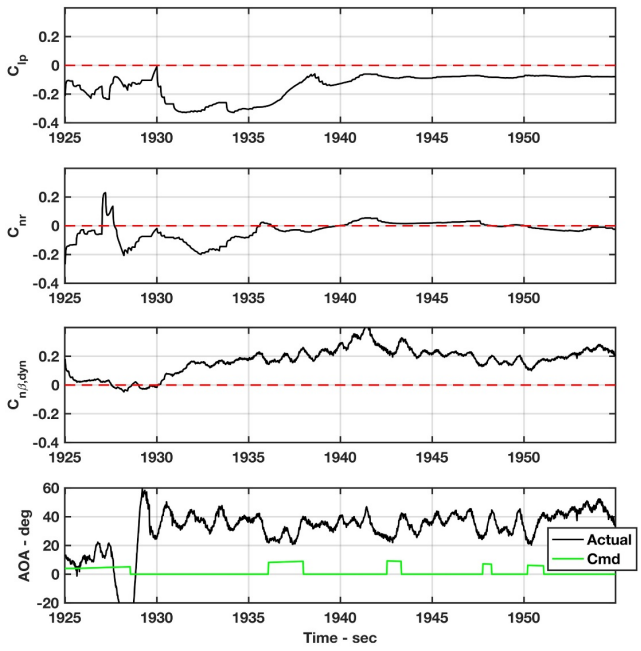

(b) Woodstock aircraft.

Fig. 10. Time histories of in-flight estimated stability parameters. Positive values of C_{lp} and C_{nr} and negative values of $C_{n\beta,dyn}$ indicate a potential instability.

Due to the limitations of aerodynamic stability metrics discussed above, an alternate stability assessment approach based on control surface activity was considered. If the assumption can be made that degraded stability is indicated by control surfaces approaching deflection limits or by high and prolonged surface rates, direct monitoring of control surface activity should be considered. Fig. 11 shows flight test results of normalized surface deflection cross-plotted versus normalized surface rates for the Woodstock and E1 aircraft. For these examples control surface deflection is normalized by 85% of the physical limit and control surface rate is normalized by a selected maximum rate. The red dashed boundary represents a proposed criterion that considers both the deflection and rate. Fig. 12 shows time histories for both aircraft indicating when this criteria is exceeded. It is recognized that maximum surface rates would be expected intermittently for certain conditions or maneuvers. Therefore, a persistence criterion would be required for a practical implementation of this metric. The results shown in the figure indicate degraded stability/loss of control during most of this flight for the Woodstock aircraft but normal control activity for the E1 aircraft. One advantage of this metric is that there is negligible time delay in the measurement and low uncertainty in the measured values. Based on this approach a reliable metric would likely require a synthesis of all control surface activity to indicate a potential loss of stability.

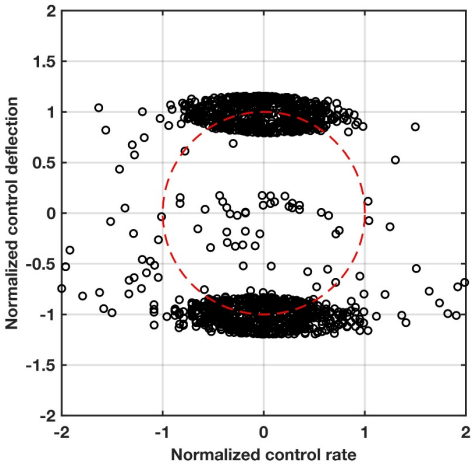

(a) Woodstock aircraft. Right wingtip control surface.

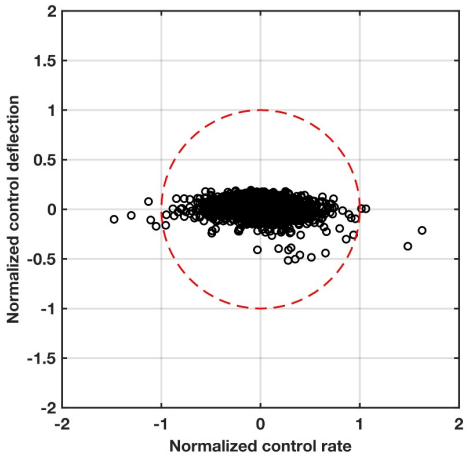

(b) E1 aircraft, flight 8. Right aileron control surface.

Fig. 11. Example results of normalized control surface deflection and rate. Red dashed line indicates proposed criteria.

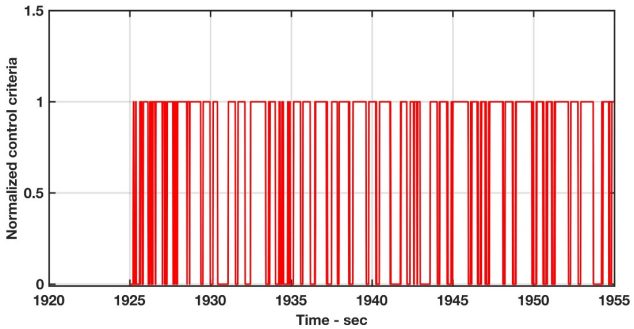

(a) Woodstock aircraft. Right wingtip control surface.

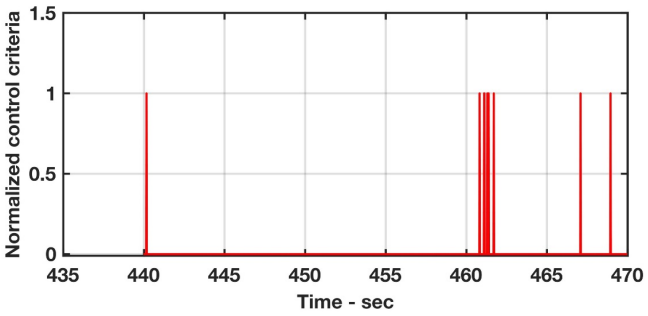

(b) E1 aircraft, flight 8. Right aileron control surface.

Fig. 12. Time histories of proposed control-based stability monitoring. Value greater than zero indicates exceedance.

Autonomous Landing

The E1 aircraft was used to demonstrate in-flight energy management and autonomous landing accuracy based on in-flight, self-learning glide performance. A flight profile was designed to emulate the Woodstock fligh profile by starting the onboard algorithms during a dive simulating balloon release followed by navigating to the first waypoint. The laser altimeter was not installed in this vehicle, so the autoflare algorithm could not be evaluated during this test. Figure 13 presents a flight profile showing the aircraft entering the loiter pattern and flying the landing approach using the energy management approach previously described. In this example, waypoint skipping was demonstrated when the altitude was low prior to the base turn but crossed the target altitude within 5 ft during the turn for the final leg of the approach. Figure 14 shows the L/D ratio which was used to compute the commanded flight path angle for landing and the corresponding 1g trim airspeed computed in-flight. For the purposes of this test, the estimated values of L/D and trim airspeed were held constant throughout the autoland sequence rather than allowing them to update in real-time. Further flight testing is recommended to assess the effects of real-time updates on landing performance.

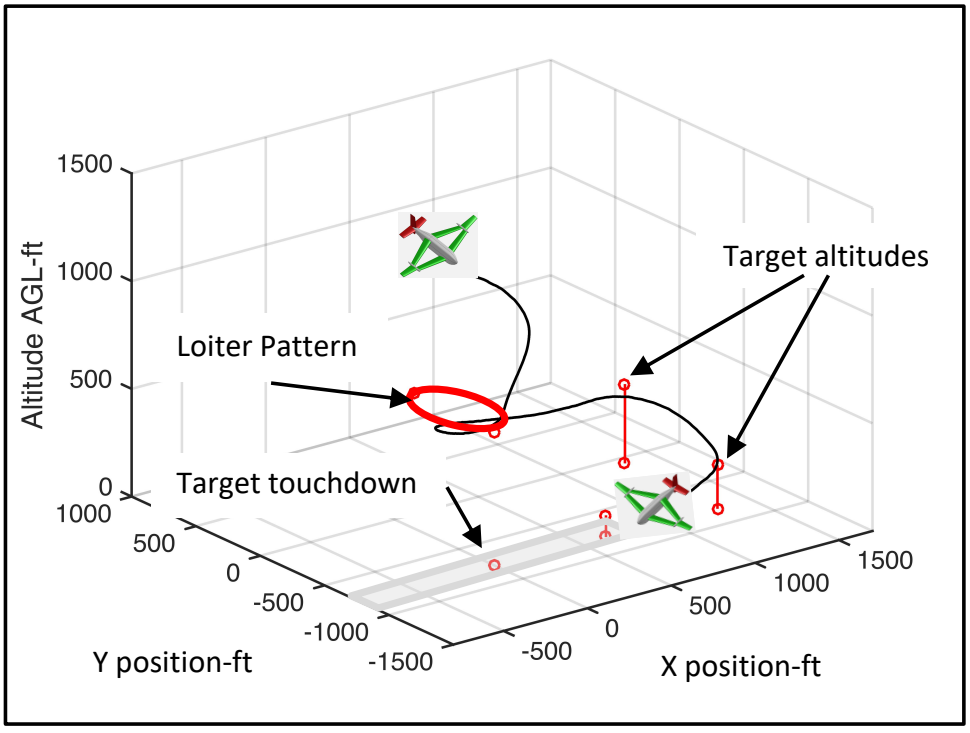

Fig. 13. Autoland flight demonstration. E1 aircraft, flight 8.

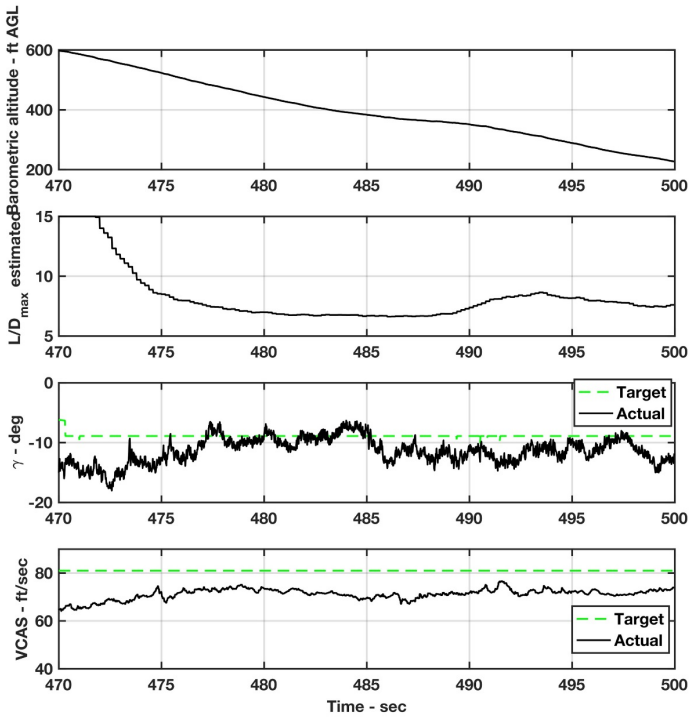

Fig. 14. In-flight estimated landing parameters for autoland flight test. E1 aircraft, flight 8. Dashed green lines are inflight estimated values.

V. Summary and Future Research

This paper has presented a functional description of the guidance system for the NASA Learn-to-Fly project. The guidance system primarily was designed as an executive algorithm, where primary commands to the inner-loop controllers were coordinated to enable autonomous flight within defined test range boundaries while executing self-learning control through a range of flight conditions and landing. The scope of the guidance function development included test range boundary definitions, flight operations procedures and onboard control algorithms to enable autonomous waypoint navigation, and flight envelope management. Development of the L2F guidance algorithms was accomplished using simulation tools where software for the real-time modeling and control algorithms and system characteristics were integrated with low-fidelity models of surrogate flight vehicles.

A discussion of flight test considerations has been presented, unique to the L2F test environment, that are not normally required in conventional flight testing of fixed-wing vehicles. A significant challenge in this effort was flight test risk mitigation, specifically test range requirements and loss of control prevention, due to unknown vehicle flight characteristics prior to flight. The flight test program employed several approaches to risk mitigation including the development of test range boundaries, and impact point prediction for development of flight termination criteria. Flight test validation and feasibility assessment was provided by test flights on two different vehicles.

A primary goal of the L2F project was to demonstrate the feasibility of self-learning concepts for flight vehicle development. Based on limited flight test results, the ability to effectively operate and test self-learning vehicles was demonstrated. The potential for real-time self-learning for autonomous navigation and landing, energy management, and envelope limiting was also demonstrated. A key finding was the importance of autonomous/self-learning envelope expansion capability for vehicles where no stability and control characteristics are known prior to flight. Additional research is recommended to further develop in-flight stability monitoring concepts and algorithms for autonomous envelope limiting to further enable future L2F flight test research.

Acknowledgements

Funding for the Learn-to-Fly project was provided by the NASA Convergent Aeronautics Solutions (CAS) project. The contributions of the L2F test team to the airframe development, real-time modeling and control algorithm development, and flight test efforts are gratefully acknowledged.

References

[1] Heim, E. H., Viken, E. M., Brandon, J. M., and Croom, M. A., "NASA's Learn-to-Fly Project Overview", AIAA Atmospheric Flight Mechanics Conference, AIAA Aviation Forum, June, 2018 (to be published).
[2] Riddick, S. E., Busan, R. C., Cox, D. E., and Laughter, S. A., "Learn-to-Fly Test Setup and Concept of Operations", AIAA Atmospheric Flight Mechanics Conference, AIAA Aviation Forum, June, 2018 (to be published).
[3] Morelli, E. A., "Practical Aspects of Real-Time Modeling for the Learn-to-Fly Concept", AIAA Atmospheric Flight Mechanics Conference, AIAA Aviation Forum, June, 2018 (to be published).
[4] Snyder, S. M., Bacon, B. J., Morelli, E. A., Frost, S. A., Teubert, C. A., and Okolo, W. A., "Online Control Design for Learn-to-Fly", AIAA Atmospheric Flight Mechanics Conference, AIAA Aviation Forum, June, 2018 (to be published).
[5] Cunningham Kevin, Cox, David E., Foster, John V., Riddick, Stephen E., and Laughter, Sean A.,"AirSTAR Beyond Visual Range UAS Description and Preliminary Test Results", AIAA-2016-0882, Jan. 2016.